Current Biology, Vol. 12, 483–487, March 19, 2002, ©2002 Elsevier Science Ltd. All rights reserved. PII S0960-9822(02)00718-2

Spatiochromatic Properties of Natural Images and Human Vision

C.A. Párraga,[1,4] T. Troscianko,[2] and D.J. Tolhurst[3]
[1]Department of Experimental Psychology
University of Bristol
8 Woodland Road
Bristol, BS8 1TN
United Kingdom
[2]School of Cognitive and Computing Sciences
University of Sussex
Brighton, BN1 9QH
United Kingdom
[3]The Department of Physiology
University of Cambridge
Downing Street
Cambridge, CB2 3EG
United Kingdom

Summary

The human visual system shows a relatively greater response to low spatial frequencies of chromatic spatial modulation than to luminance spatial modulation [1]. However, previous work [2, 3] has shown that this differential sensitivity to low spatial frequencies is not reflected in any differential luminance and chromatic content of general natural scenes. This is contrary to the prevailing assumption that the spatial properties of human vision ought to reflect the structure of natural scenes [4–6]. Now, colorimetric measures of scenes suggest that red-green (and perhaps blue-yellow) color discrimination in primates is particularly suited to the encoding of specific scenes: reddish or yellowish objects on a background of leaves [7–10]. We therefore ask whether the *spatial*, as well as *chromatic*, properties of such scenes are matched to the different spatial-encoding properties of color and luminance modulation in human vision. We show that the spatiochromatic properties of a wide class of scenes, which contain reddish objects (e.g., fruit) on a background of leaves, correspond well to the properties of the red-green (but not blue-yellow) systems in human vision, at viewing distances commensurate with typical grasping distance. This implies that the red-green system is particularly suited to encoding both the spatial and the chromatic structure of such scenes.

Results and Discussion

Figure 1 shows two very different examples of photographs of natural scenes; Figure 1A shows a landscape view of a British garden, and Figure 1B shows a closeup of a single ripe tomato seen against foliage. We calculated how the human L, M, and S (for long-, medium-, and short-wavelength-sensitive) cones would have responded at each point in each of the scenes, and we then calculated the spatial form of the luminance signal and the red-green and blue-yellow chromatic signals within the human visual system. A simple way of representing the amount of Fourier amplitude at different spatial frequencies in complex images is given by plotting the spectral slope of the signal. If the amplitudes of all the Fourier components of natural images are plotted on logarithmic axes against their spatial frequencies, one obtains an approximately straight-line plot, with a slope (α) around -1.2 [11, 12]. This slope is said to have evolutionary importance, since our visual system is optimized for processing the spatial information in natural scenes at this particular value [13], and there are theoretical reasons why there should be a strong relationship between α and cortical receptive field profiles [6]. Essentially, a match between the scene content and the visual system's response maximizes the signal-to-noise ratio of the neural representation. Figure 2A shows just such plots for the luminance and for the two chromatic signals for the garden scene of Figure 1A. It is clear that the slopes (α) are very similar for the three graphs, though it should be noted that the magnitude of the amplitude in the red-green signals was considerably less than in the blue-yellow signal (the luminance has to be plotted on a different scale). Since human color vision is biased more toward low spatial frequencies than is luminance vision, we might have expected the spectral slope of the chromatic spatial signals to be steeper than that of the luminance signal, given that a steeper spectral slope gives a greater weight to low spatial frequencies. The failure to find such an effect for the scene in Figure 1A confirms the earlier study of Párraga et al. [2] using hyperspectral images.

In that earlier study, the spatiochromatic properties of 29 natural scenes were analyzed, but they mostly consisted of views of foliage and gardens such as that in Figure 1A. However, there is a body of literature [7–10] that suggests that primate (including human) color channels may optimally encode the chromatic difference between red or yellow fruit and green foliage (or, indeed, of any red or yellow objects on green foliage), so it is important to examine the spectral slopes of similar natural images; i.e., of fruit in foliage, similar to those used by these researchers. Figure 2B shows plots of the Fourier amplitude spectra of the luminance and the two chromatic spatial signals of the closeup image of the ripe tomato of Figure 1B. It is indeed clear that the spectral slope (α) of the red-green spatial signal is now steeper than those of the luminance or blue-yellow spatial signals; the total amplitude for the red-green signal is, not surprisingly, much greater than for the general garden scene.

Figure 3 shows the generality of our finding that the amplitude spectrum of the red-green spatial signal is steep for closeup images of reddish objects viewed against foliage. Figure 3A plots the ratio between the spectral slopes obtained for the luminance spatial signal and the red-green spatial signal for each scene as a function of how many "red" pixels (in %) there were in the scene (see the Experimental Procedures for a definition of a "red" pixel). It can be seen that the results

[4]Correspondence: alej.parraga@bristol.ac.uk

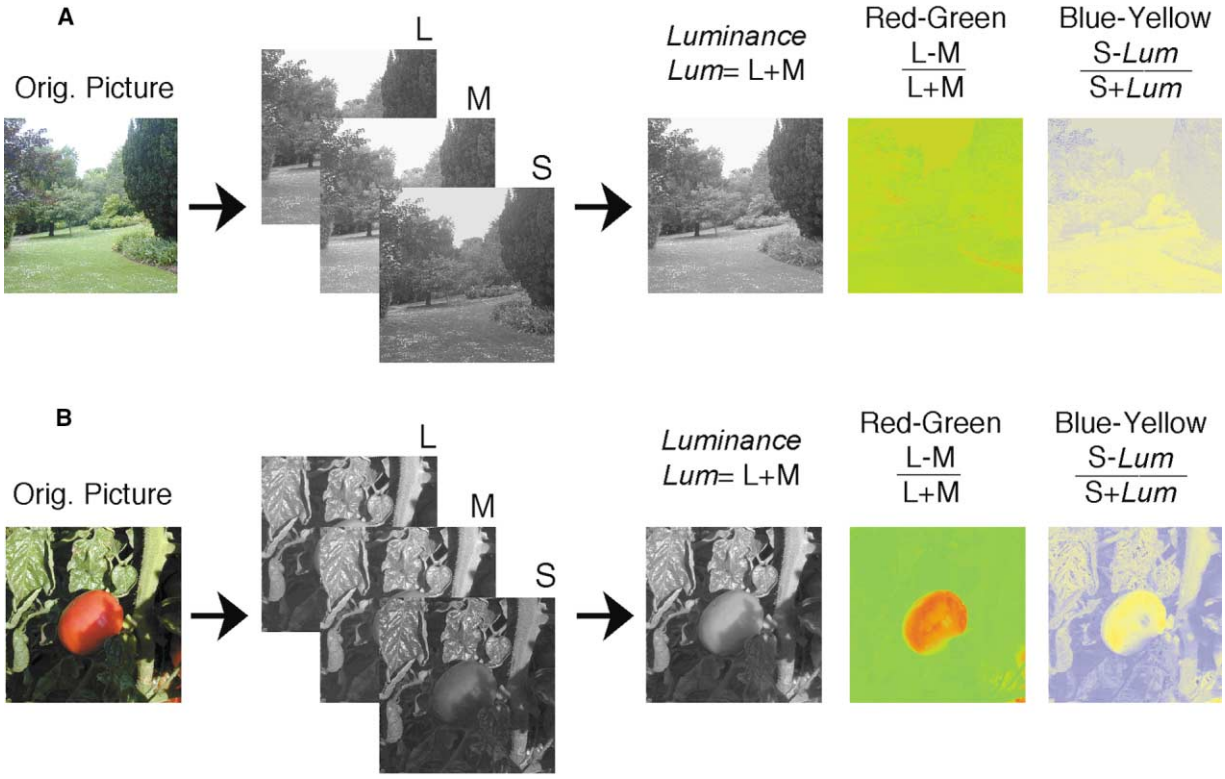

Figure 1. Decomposition of an Original Image into L, M, and S Cone-Sampled Images, and the Derivation from These of the Three Final Representations: Luminance, Red-Green Chromatic, and Blue-Yellow Chromatic

(A) The analysis for a picture similar to those used in previous work.

(B) The same analysis for a picture of a red tomato on a background of green leaves.

Note that the luminance and chromatic representations have been scaled in order to maximize the available dynamic range. In fact, the red-green representation in (A) actually has much less amplitude than shown. In (B), the variability of color and brightness within the background of leaves is removed, making the uniform red tomato pop out. Note that the divisive term in the calculation of the red-green and blue-yellow representations means that the pixel values range between −1 and 1, while the scaling factor for the luminance representation is essentially arbitrary.

for all scenes follow a similar trend and are differentiated on the basis of red pixel content (note that scenes consisting of a background of foliage and a reddish object such as fruit appear on the right side of the graph, while scenes of landscapes with no red objects appear on the left). The important predictor of slope ratio appears to be the proportion of red pixels on the leafy background. In general, the spectral slope of the red-green signal is greater than that of the luminance signal whenever the scene contains many red pixels. When those red pixels are grouped together to represent a single object (like Figure 1B), the slopes of the spectra are especially steep and the slope ratio deviates most from unity. When the pixels are clustered into several groups, representing several distinct fruits, the slopes of the amplitude spectra are not as steep, but the slope for the red-green signal is always steeper than for the other two signals.

In contrast, Figure 3B shows that the spectral slope of the blue-yellow spatial signal does not differ systematically from that of the luminance signal. There is no evidence in this set of images to suggest that there is any advantage in the bias of the human blue-yellow system to low spatial frequencies. There may be other constraints on the development of the spatial characteristics of blue-yellow color vision in primates. For example, it is possible that low sensitivity to high blue-yellow spatial frequencies is a consequence of chromatic aberration in the eye and/or the sparse array of short-wave sensitive cones (see Conclusions).

If the human contrast sensitivity function (csf) is optimized to match the spatial frequency content of natural images, then we should find that chromatic images contain more low spatial frequency amplitude than luminance images, or in other words, that the ratio ($\alpha_{lum}/\alpha_{chrom}$) should be less than unity. We calculated the optimal value for this ratio, assuming optimal capture by the contrast sensitivity functions [1]. This optimal value is around 0.76 (see the Experimental Procedures). Figure 4 plots the ratio of the spectral slopes (for the luminance image and the red-green chromatic image) against the distance of the main objects in the scene from the camera. It is clear that the distant scenes like Figure 1A have slope ratios around unity, but close views of red objects against foliage have lower slope ratios. The ratio matches the calculated optimal value for the human csf at a viewing or grasping distance of about 0.4 m. This estimate does require some assumptions and would be influenced, for instance, if we had taken images with a different focal length of camera lens. However, our estimate of 0.4 m

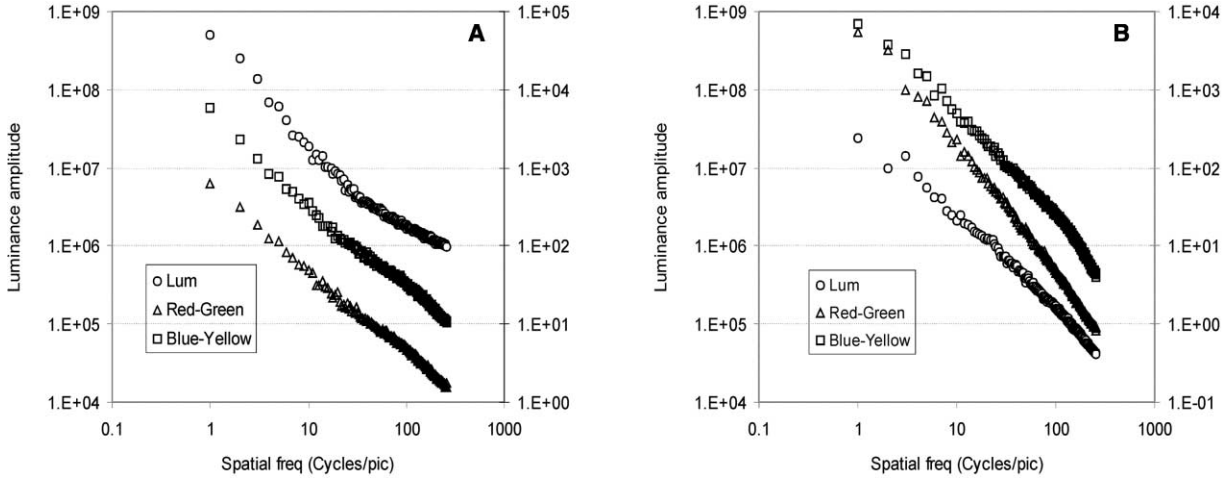

Figure 2. Examples of the Luminance and Chromatic Spectral Slopes of Our Natural Scenes

Circles correspond to the luminance, triangles correspond to the red-green signals, and squares correspond to the blue-yellow signals. The Fourier amplitude (averaged across orientation) is shown as a function of spatial frequency for the luminance and chromatic representations of the outdoor image with various kinds of foliage (Figure 1A) and the tomato image (Figure 1B). When logarithmic coordinates are used on both axes, the data fall on straight lines whose slopes are called the spectral slope (α), which usually has a value in the range -0.7 to -1.6. Different y scales are used for the luminance data (left scale) compared to the chromatic data (right scale), because of the different scaling in the pixel values of the two kinds of representation.

(A) The plot shows no difference between the luminance and chromatic slopes.

(B) The plot shows a steeper slope for the red-green image than for the blue-yellow and luminance images.

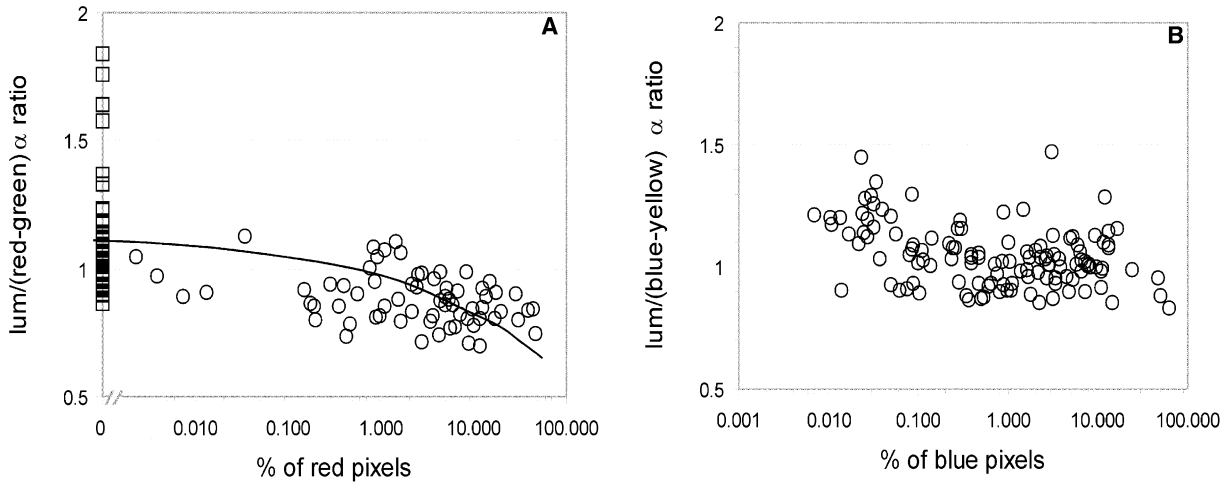

Numerical means and stds	normal scenery (not including red objects) n= 58		All other images (including red objects) n= 66	
	mean	std	mean	std
Lum/RG_chrom slope ratio =	1.105	0.222	0.880	0.098
Lum/BY_chrom slope ratio =	1.043	0.143	1.049	0.108
Lum slope =	-1.108	0.198	-1.162	0.178
RG_chrom slope =	-1.016	0.160	-1.331	0.226
BY_chrom slope =	-1.068	0.160	-1.119	0.201

Figure 3. The Ratio of the Spectral Slopes of the Luminance and Chromatic Representations, for Different Image Types, as a Function of the Percentage of Pixels Signaling the Presence of a "Red" Object

(A and B) The background always consisted of green foliage. The data plotted on the left correspond to pictures of scenery without a strong presence of red objects (normal scenery: distant landscapes or closeups of foliage), and their $\alpha_{lum}/\alpha_{chrom}$ slope ratio near unity is consistent with previous findings [2]. The squares correspond to scenes with no presence of "red" pixels (i.e., they are plotted on the *y* axis). The line in (A) represents the approximate data trend and reflects the fact that the average $\alpha_{lum}/\alpha_{chrom}$ slope ratio for normal scenery is about 1.1 (see Table S1). Table S1 shows the numerical means and standard deviations of the slope ratios. Note that there is a tendency for the slope ratio to fall with increasing proportion of red content for the red-green images (A), but not for the blue-yellow images against the proportion of blue content (B). A high red content indicated the presence of fruit or a similar object.

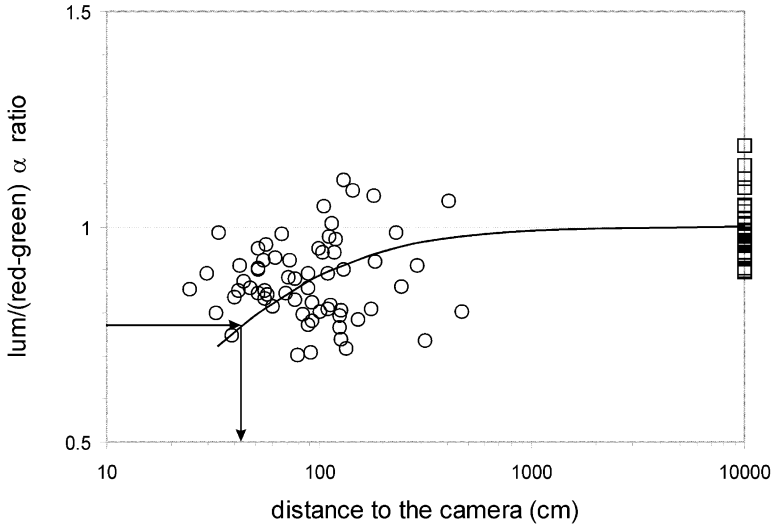

Figure 4. The Relationship between the Ratio of the Spectral Slopes and the Distance from the Camera to the Main Object in Each Scene, Assuming a 13.6° Total Subtense

The squares represent "distant landscape" scenes, i.e., scenes in which objects (trees, rocks, bushes, etc.) were numerous and their location was further away than 50 m. The line represents the data trend and reflects the fact that average values of $\alpha_{lum}/\alpha_{chrom}$ slope ratio are equal to 1.0 for these landscapes. The log *x* axis was chosen to best show the geometrical relationship between the variables. Distances were estimated from the real size of the object (in cm), the size of the object on the final picture (in pixels), and the subtended angle of our pictures. The optimal viewing distance (where the slope ratio is around 0.78) is therefore approximately 40 cm. It could be conservatively argued that this calculation suggests that the optimal viewing distance is of the order of magnitude of typical primate grasping distance. Since we are only making order-of-magnitude claims here, the trendline was drawn by eye.

will be close to the distance at which the human red-green spatiochromatic system will be optimized for identifying red or yellow fruits against foliage.

Although our stimuli were pictures of fruit and leaves obtained in England, and not in a forest in which primate color vision and relevant vegetation are thought to have coevolved, a wide variety of types of scenes can match the human contrast sensitivity data well. For this reason, we believe that this pattern of results would extend to any similar imaging situation, be it located in another garden or in a relevant forest. This also implies that we cannot argue for the optimality of encoding of any particular type of reddish or yellowish object on a leafy background; any such object would do just as well, whether it be a red fruit [7–9], a reddish human face, or a leaf that is more yellow than the rest [10]. Thus, these results do not specify exactly which kinds of images and tasks were associated with the evolution of color vision in primates. We simply find that human (and presumably other primate) color vision is efficient at encoding images of reddish or yellowish fruit, viewed up close, against a leafy background. It may be that (as with the sampling of blue light) the low-frequency bias of the red-green system has been determined by factors such as chromatic aberration, but we find that such a bias would not disadvantage a foraging primate, and it might even aid the task of picking ripe fruit or leaves.

Conclusions

Our results therefore suggest that it is the red-green system whose spatiochromatic properties are optimized for detecting reddish or yellowish objects against a background of foliage; while the blue-yellow system retains the same spectral slope as the luminance system. Returning to Figure 1B, we can see why this might be. The red-green system eliminates the dappled background of leaves [10], giving a representation of a *uniform* fruit on a *uniform* background. This allows the fruit to "pop out" from the background. Perhaps surprisingly, the blue-yellow image does not provide a uniform background, possibly since shadow regions have indirect illumination from skylight (which is blue), but also because green leaves differ in their blueness [10]. This behavior of the blue-yellow system implies that it is not optimized for detecting objects in foliage. Many questions remain. For example, the human blue-yellow system also has a low-pass transfer characteristic, and yet this seems to have little connection with the efficient detection of fruit or any other target that we have discovered. It may be that there is a different class of images that will reveal similar optimization of the blue-yellow system, or there may be other constraints on the spatiochromatic properties of this system, such as the sparse sampling by the mosaic of short-wavelength-sensitive cones in the retina, which may be related to the fact that short wavelengths are out of focus on the retina due to chromatic aberration. We have not investigated these issues here. We suggest that a reasonable, although clearly tentative, conclusion from the present work is that the spatiochromatic properties of the red-green system of human color vision may be optimized for the encoding of any reddish or yellowish objects on a background of foliage, at relatively small viewing distances.

Experimental Procedures

Obtaining the Images

We carefully calibrated a digital camera (Nikon Coolpix 950) so that each pixel in the (uncompressed) output image represented the capture of each of the three human cone types. The calibration process utilized a set of narrowband optical interference filters spanning the range from 400 to 700 nm, a constant-current light source, and a Topcon SR-1 telespectroradiometer calibrated against a National Physical Laboratory standard light source. This procedure removed the various nonlinearities introduced by the camera electronics, and it compensated for the spectral responses of the camera's CCD. The output of this process was a trichromatic representation of each scene giving, for each pixel, the *relative* capture ratios of the three human cone types, based on the Smith and Pokorny

[14] cone fundamentals. The three planes in these images (labeled L, M, and S) were then combined to obtain luminance and chromatic representations as shown in Figure 1. The L and M cone activations by red fruit and leaves obtained with this method were compared to similar output of the SR-1 in controlled conditions for a variety of red fruit and green leaves, and the results differed by less than 13% in all cases.

We obtained 124 images with a spatial resolution of 512 $\times$ 512 pixels $\times$ 24 bits. These were taken under different conditions of illumination (sunny and cloudy), at different distances from the objects, and with many different kinds of non-green objects among foliage (large red fruit such as apples and tomatoes; small red berries; flowers). Almost all were taken using the minimum aperture (f/11–f/11.4), i.e., the maximum depth of field available to avoid differences in focus within the same picture. A total of 66 images contained "red" pixels, and 58 did not. We defined a "red" pixel as one in which the estimated activation of the L cone was 1.5 times or more the activation of the M cone; the ratio of cone activations followed a clear bimodal distribution, with a ratio of 1.5 in the trough. A total of 27 images were of landscapes in which objects were at distances in the range of 20–500 m. A total of 32 images were closeups of plants with no red objects. All of the pictures were taken in England, in various gardens. Most of the pictures were taken with the zoom lens set to its telephoto (19–20.4 mm focal length) setting. This avoided having to bring the camera very close to the objects, thus affecting illumination. Linear perspective is somewhat affected by this procedure compared to natural viewing, but this was found not to affect the spectral slope values in any systematic way. Square images with an angular subtense of 13.6° were cropped from the rectangular images, and these were reduced to a size of 512 $\times$ 512 pixels. We checked for, and did not find, significant effects of chromatic aberration of the camera lens.

Measuring α

In order to avoid edge effects, all images had their borders smoothed with a gaussian roll-off (SD = 15 pixels). A two-dimensional fast-Fourier transform was used to derive the amplitude spectrum for a given luminance or chromatic spatial representation. The DC component was removed. Spectral slopes were measured by dividing the Fourier space into nine circularly symmetric, logarithmically spaced, one-octave spatial-frequency bands, and then averaging the Fourier content within each of the bands. The averages were then plotted against the midspatial frequency of the band on log-log coordinates, and the slope (α) of this line was calculated by linear regression. This prevented any bias due to oversampling of the high spatial frequencies. These methods are explained in greater detail elsewhere [2, 15].

Calculating the Optimal Ratio of Luminance to Red-Green Color Spectral Slopes

We compared the csfs measured for sinusoidal spatial modulations of luminance and red-green chromatic contrast [1]. The total area under the luminance csf was normalized to unity, as was the area under the equivalent csf for chromatic modulation. We divided the spatial frequency axis into logarithmic bands (coincident with the ones used for measuring α) and calculated the areas under each of the two csfs for every band. We then calculated the area ratios of luminance-csf to color-csf in each band. We found that a ratio of 0.76 in the spectral slopes ($\alpha_{lum}/\alpha_{chrom}$) gives approximately the same normalized area ratio.

Supplementary Material

Supplementary Material including further details of the methods employed to calibrate our digital camera, verify the quality of the calibration, and analyze the data is available at http://images.cellpress.com/supmat/supmatin.htm.

Acknowledgments

This work was supported by a grant from the Biotechnology and Biological Sciences Research Council (UK). We thank Ian Moorhead and Marilyn Gilmore for technical assistance and Daniel Osorio, Roland Baddeley, Iain Gilchrist, Donald MacLeod, and Rüdiger von der Heydt for helpful comments. Two anonymous reviewers made excellent suggestions for improvement.

Received: October 4, 2001
Revised: December 3, 2001
Accepted: January 14, 2002
Published: March 19, 2002

References

1. Mullen, K.T. (1985). The contrast sensitivity of human color vision to red-green and blue-yellow chromatic gratings. J. Physiol. (Lond.) *359*, 381–400.
2. Párraga, C.A., Brelstaff, G., Troscianko, T., and Moorhead, I.R. (1998). Color and luminance information in natural scenes. J. Opt. Soc. Am. A *15*, 563–569.
3. Webster, M.A., and Mollon, J.D. (1997). Adaptation and the color statistics of natural images. Vision Res. *37*, 3283–3298.
4. Barlow, H.B. (1961). Possible principles underlying the transformation of sensory messages. In Sensory Communications, W.A. Rosenblith, ed. (Cambridge, MA: MIT Press), pp. 217–234.
5. Marr, D. (1982). Vision: A Computational Investigation into the Human Representation and Processing of Visual Information (San Francisco: W.H. Freeman).
6. Field, D.J. (1987). Relations between the statistics of natural scenes and the response properties of cortical-cells. J. Opt. Soc. Am. A *4*, 2379–2394.
7. Osorio, D., and Vorobyev, M. (1996). Colour vision as an adaptation to frugivory in primates. Proc. R. Soc. Lond. B *263*, 593–599.
8. Regan, B.C., Julliot, C., Simmen, B., Vienot, F., Charles-Dominique, P., and Mollon, J.D. (1998). Frugivory and colour vision in *Alouatta seniculus*, a trichromatic platyrrhine monkey. Vision Res. *38*, 3321–3328.
9. Sumner, P., and Mollon, J.D. (2000). Catarrhine photopigments are optimized for detecting targets against a foliage background. J. Exp. Biol. *203*, 1963–1986.
10. Dominy, N.J., and Lucas, P.W. (2001). Ecological importance of trichromatic vision to primates. Nature *410*, 363–365.
11. Field, D.J. (1989). What the statistics of natural images tell us about visual coding? SPIE - Human vision, visual processing and digital displays *1077*, 269–276.
12. Tolhurst, D.J., Tadmor, Y., and Chao, T. (1992). Amplitude spectra of natural images. Ophthalmic Physiol. Opt. *12*, 229–232.
13. Párraga, C.A., Troscianko, T., and Tolhurst, D.J. (2000). The human visual system is optimized for processing the spatial information in natural visual images. Curr. Biol. *10*, 35–38.
14. Smith, V.C., and Pokorny, J. (1975). Spectral sensitivity of the foveal cone photopigments between 400 and 500 nm. Vision Res. *15*, 161–171.
15. Brelstaff, G.J., Párraga, C.A., Troscianko, T., and Carr, D. (1995). Hyperspectral camera system: acquisition and analysis. Geographic information systems, photogrammetry, and geological/geophysical remote sensing. SPIE - Human vision, visual processing and digital displays *2587*, 150–159.